Chapter 2
Laboratory Testing Methods of Cavitation Erosion

Georges L. Chahine, Jean-Pierre Franc and Ayat Karimi

Abstract This chapter presents in detail several cavitation erosion testing methods commonly used in the laboratory. The vibratory cavitation apparatus (G32) is described with its two variants, the direct method using a specimen attached to the vibrating tip of the ultrasonic horn and the alternative method using a fixed specimen facing the horn tip. In the cavitating jet apparatus (G134 and its variants), a jet is discharged at high pressure and velocity in a cell whose pressure may be controlled to adjust the cavitation number. This results in a shear type cavitation whose aggressiveness may be enhanced by a proper design of the nozzle shape and piping assembly. A high-speed cavitation tunnel equipped with a radial divergent test section is also presented. This particular test section generates an unsteady cavity attached to the nozzle exit with cavitation erosion damage concentrated in the cavity closure region. Usual testing procedures together with typical erosion patterns and mass loss results obtained in such facilities are also presented.

2.1 Introduction

Proper evaluation of new materials for their resistance to cavitation erosion requires a comprehensive effort addressing both the intensity of the cavitation field and the resistance of the material. In the absence of historical data on the

G. L. Chahine (✉)
DYNAFLOW, INC., 10621-J Iron Bridge Road, Jessup, MD, USA
e-mail: glchahine@dynaflow-inc.com

J.-P. Franc (✉)
LEGI, Grenoble, France
e-mail: jean-pierre.franc@legi.grenoble-inp.fr

A. Karimi (✉)
EPFL, Lausanne, Switzerland
e-mail: ayat.karimi@epfl.ch

K.-H. Kim et al. (eds.), *Advanced Experimental and Numerical Techniques for Cavitation Erosion Prediction*, Fluid Mechanics and Its Applications 106,
DOI: 10.1007/978-94-017-8539-6_2,

performance of a new material in the target cavitating flow fields, experimental studies in the laboratory offer a convenient means of assessing the cavitation erosion performance.

Field erosion studies have been conducted for hydraulic turbines and pumps (e.g. [1–5]), but for marine applications, small scale laboratory tests are more common. These laboratory experimental studies aim at obtaining within the required short time periods an evaluation of the cavitation resistance of the new material, whereas in the real field cavitation erosion may occur after a long duration of exposure.

Such accelerated erosion test techniques include the utilization of ultrasonic vibration devices to generate the cavitation [6–8], cavitation flow loops with strong flow separation, vortex or venturi effects [9–11], rotating discs and submerged cavitating jets [12–15], and other methods. There are also attempts to test model propellers in water tunnels [16].

Some of these techniques are standardized and follow the American Society for Testing and Materials (ASTM) Standards [17]. The ultrasonic technique and the liquid jet technique are the two most popular laboratory techniques for testing cavitation erosion characteristics of materials.

In this chapter, three different laboratory testing methods and equipments are presented in detail, and are used to generate the erosion data presented in Part 1 of this book. They are vibratory devices (ASTM G32), cavitating liquid jets (ASTM G134), and a high-speed cavitation tunnel.

2.2 Vibratory Cavitation Apparatus (ASTM G32)

In ultrasonic cavitation tests, the cavitation is generated by a vibratory device employing a magnetostrictive ultrasonic horn (Fig. 2.1). The high frequency oscillations of the horn, typically tens of kilohertz, induce cyclic formation of very high and very low pressures, which generate high negative tension in the liquid.

This can be understood easily if one considers the acoustic field generated by the imposed amplitude motion of the tip of the horn given by:

$$X(t) = A\,\cos(2\pi f\,t), \tag{2.1}$$

where $X(t)$ is the vertical position of the tip of the horn at instant t, A the amplitude and f the frequency of the tip vibratory oscillations.

The resulting acoustic pressure is given by:

$$p = \rho_l c_l \dot{X} = -2\pi f \rho_l c_l A\,\sin(2\pi f\,t), \tag{2.2}$$

where ρ_l is the liquid density and c_l is the sound speed in the liquid.

Typically, the vibratory device operates at 20 kHz and the amplitude of the horn tip motion, A, is maintained at 25 μm with the help of a bifilar microscope. This gives for water:

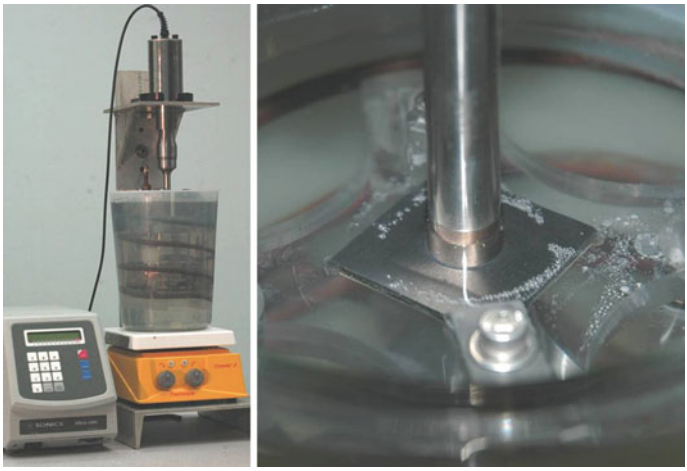

Fig. 2.1 Ultrasonic cavitation erosion test setup at DYNAFLOW. The ultrasonic horn tip vibrates at 20 kHz and generates cavitation bubbles around the tip. The *right picture* shows the alternative G32 configuration. The sample is placed in the square support plate below the cylindrical horn. The *reddish tip* is the Titanium "button". Cavitation under the horn is difficult to see as it is limited to the gap between the "button" and the sample. The *white spots* are bubbles generated by the vibrations at the free surface of the container and at the periphery of the sample holder

$$p = -4.7 \times 10^6 \sin(2\pi f t) \text{ Pascals.} \tag{2.3}$$

Since the amplitude of the pressure oscillations is much larger than the ambient pressure (actually 47 atmospheres), this results in pressure drops during the negative pulse cycle much below the critical pressure of most liquids (see Sect. 1.1.3).

A sample "button" of the material being tested is affixed to the end of the horn and is subjected to the cavitation resulting from the vibration of the horn. A hemispherical cavitation cloud forms at the exposed face of the sample and executes severe dynamics resulting in bubble cloud growth and collapse. The ASTM G32-09 [17, 18] specifies the sample diameter, 16 mm, the vibration frequency, 20 kHz, and amplitude, 50 μm peak-to-peak, and the shape and size of the container in order to minimize variations among different tests and laboratories due to acoustic interaction between transducer and container. A 2,000 ml beaker filled with distilled water and with the tip of the horn submerged 8 mm beneath the free surface is required. In addition, the temperature is controlled by immersing the beaker in a water bath maintained at 25 ± 2 °C.

In an "alternative" G32 test configuration [12, 19] (also known as the stationary specimen method), a stationary material sample is placed at a small distance, typically 0.5 mm, below the vibrating horn tip made of a cavitation resistant button (e.g. Titanium). Deviations from the ASTM G32 method have to be documented. The cavitation erosion tests presented in Chap. 5 used a sample diameter of 12.7 mm instead of 16 mm recommended by the ASTM for both the direct and alternative methods. The alternative G32 method is especially useful for testing

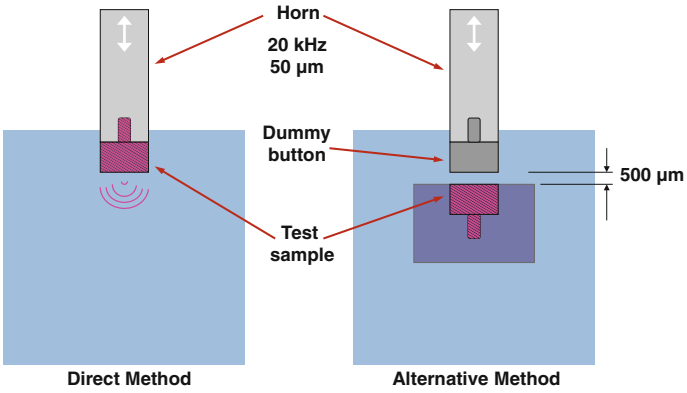

Fig. 2.2 Sketches of the test setups for the ultrasonic cavitation ASTM G32 direct method (*left*) and the alternative method (*right*). In the direct method a hemispherical microbubble cloud is formed under the sample and collapses quasi spherically onto the sample. In the alternative method, the cloud is cylindrical and is confined between the sample and a dummy button, and collapses quasi-cylindrically

Fig. 2.3 Aluminum alloy Al 7075 samples tested at DYNAFLOW by ASTM G32 direct method (*left*) and alternative method (*right*). Both pictures are shown for 900 min of exposure to cavitation. (Button samples diameter: 12.7 mm)

materials difficult to be made into threaded buttons. Sketches of both setups are shown in Fig. 2.2.

Figure 2.3 shows samples with typical patterns of advanced erosion and mass loss tested by the two ultrasonic cavitation methods. The erosion patterns are significantly different, with the direct method showing a large eroded area concentrated mainly in the central part of the sample, while the alternative method shows a more spread erosion pattern. This is because the shape of the bubble cloud is different between the two schemes. In the direct G32 method the cavitation

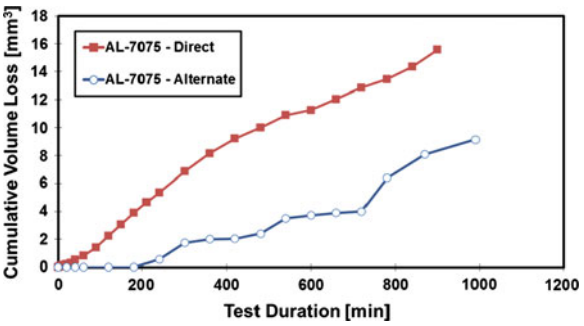

Fig. 2.4 Comparison of material erosion progression on Al 7075 samples tested at DYNAFLOW using both the ASTM G32 direct method and the alternative method. Erosion in the alternative method progresses much slower than with the direct method

cloud collapses in a hemispherical way towards the tested sample (see Fig. 2.2 left), while in the alternative method, the cavitation bubble cloud collapses in a cylindrical way (see Fig. 2.2 right). Cavitation clouds collapsing cylindrically were found to be much less erosive than the hemi-spherically collapsing cavitation clouds [12, 19].

Mass loss versus time curves on the same material (aluminum alloy Al 7075) for the two methods are presented in Fig. 2.4, which illustrates a mass loss rate by the direct method being almost twice that of the alternative method.

The conventional test procedure using the ultrasonic vibrating horn method is to expose the sample to cavitation for a selected period of time, interrupt the test, remove the sample, and record weight to enable calculation of weight loss as a function of time. The sample is then returned to the exact same position on the horn for additional time intervals of erosion. Other erosion characteristics such as volume of erosion imprint, maximum width and depth can also be recorded, together with photographs of the evolution of the eroded region as a function of time.

Erosion tests using ultrasonic cavitation provide reproducible cavitation within a laboratory environment, but the cavitation thus generated is different from that on a propeller or a rudder in a number of ways. The cavitation bubbles are of nearly uniform sizes and are excited by the horn at a fixed frequency, while real cavitation fields have a distribution of bubble nuclei sizes and cavitation forms and vastly different exciting frequencies. The ultrasonic test does not include the effects of bubble nuclei captured by turbulent vortex filaments, break-up of cavities, and presence of liquid flow that interacts with the bubbles. The most important discrepancy is the presence in the ultrasonic method of a cavitation bubble cloud always at the same location.

2.3 Cavitating Liquid Jets (ASTM G134 and Variants)

Cavitating jets have been used extensively for materials testing because of the flexibility these jets provide to control and dial the cavitation intensity. The American Society for Testing and Materials (ASTM) established a standard

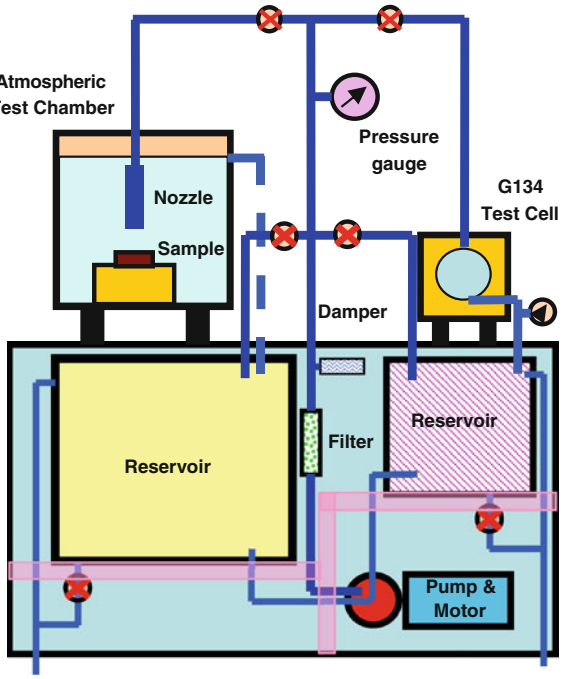

Fig. 2.5 Sketch of the "7 ksi (48 MPa) − 5 gpm (0.3 l/s)" DYNAFLOW cavitating jet test loops. This loop enables selection between open atmospheric pressure tests and the G134 test, where both ambient pressure and temperature in the test section can be controlled (0.1 MPa $< P_{amb} <$ 2 MPa, $T <$ 300 °F)

method using specific conditions and orifice type under the G134 in 1995 [20]. Cavitation intensity produced by cavitating jets can be varied in a wide range through adjustment of the type of the jet, the jet velocity, the jet diameter, the jet angle, the standoff distance, and the ambient pressure in which they are discharged [14]. The jet pressure can be as high as 300 MPa for some applications. This flexibility makes a cavitating jet a useful research and testing tool to study parametrically the effect of cavitation intensity on material behavior.

Compared to the ultrasonic horn testing (G32), the cavitation generated by a cavitating jet provides more realistic cavitation bubble clouds than that by ultrasonic horn, with distribution of various size micro bubbles, shear flows with vortices, and dense bubble clouds, which collapse on the sample. With the control of the operating pressure, the jet angle, and the standoff, the testing time can be controlled to provide either quick erosion for an initial screening or accelerated erosion more relevant to the real flows.

The cavitating jet erosion test setup used in the studies presented in Chaps. 3, 4 and 5 is sketched in Fig. 2.5. The test facility has two testing loops sharing one pump, i.e. only one loop is used at a time by shutting down the other loop using valves. The first flow loop that circulates water through the left side of the setup consists of a cavitating jet nozzle (CAVIJET®), a sample holder, an atmospheric test chamber, a water reservoir, and a pump. A sample holder is used to ensure that the sample can be taken out for measurements and then placed back precisely at the same location to continue testing.

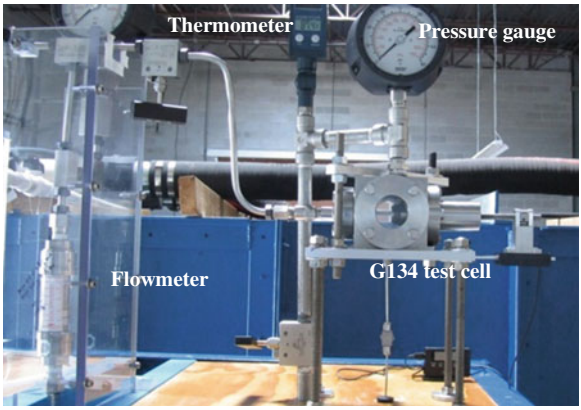

Fig. 2.6 Picture of the G134 "7 ksi (48 MPa) – 5 gpm (0.3 l/s)" test chamber loop

The second flow loop that circulates test liquid through the right half of the setup consists of a cavitating nozzle conforming to G134 specification (0.4 mm orifice diameter), a sample holder, a pressurized test cell, a water reservoir, and a pump. When the cavitation number needs to be controlled or maintained for different jet pressures, the jet is discharged in a pressure controlled cell, where the ambient pressure can be increased (see Fig. 2.6). This is the case for the G134 test cell setup shown in Fig. 2.5.

Different types of jets can be tested for their effect on cavitation erosion. In a conventional submerged jet (see Fig. 2.7 left), cavitation is generated in the turbulent shear layer between the high speed jet and the surrounding liquid. This results in a random distribution of elongated cavitation bubbles with some tendency to organize [21]. This tendency can be harnessed and passive acoustic enhancement can be achieved by proper design of the nozzle shape and piping assembly to result in much more erosive structured cavitating jet (see Fig. 2.7 right) [22, 23]. In this case, vorticity is collected in toroidal vortical structures, whose collapse is intense [24]. Unstructured conventional cavitating jets were used in the studies presented in Chaps. 3, 4 and 5.

For conventional materials erosion testing, where relative performance between samples is assessed, the jet and the sample are submerged in a water tank open to the atmosphere and relative erosion testing is conducted. Under these conditions, the cavitation number is very low and can be defined for cavitating jet as:

$$\sigma_{jet} = \frac{P_{tank} - P_v}{P_{jet} - P_{tank}} \ll 1, \tag{2.4}$$

where P_{tank} is the pressure in the test tank where the sample is located and P_{jet} is the pressure upstream of the nozzle orifice.

A photograph showing a typical setup of the jet nozzle and the sample in its holder is shown in Fig. 2.8. The overall test procedure is similar to that used in the G32 tests other than using a cavitating jet. A normal test procedure for a sample is as follows: (a) the sample is exposed to the cavitating jet for a predetermined

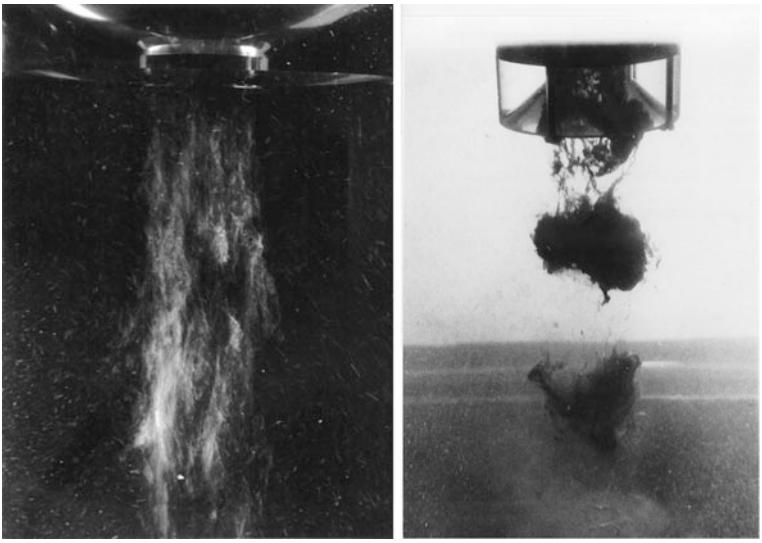

Fig. 2.7 Conventional CAVIJET® cavitating jet (*left*) and structured cavitating jet generated by a STRATOJET® (*right*). Both pictures were taken using large scale nozzles geometrically scaled up while conserving cavitation number and Strouhal number. The *left* CAVIJET® nozzle had an orifice diameter of 2.5 cm, while the *right* STRATOJET® orifice had a diameter of 1 cm. The cavitating vortex rings in the STRATOJET® were emitted with a frequency corresponding to a Strouhal number of 0.3 at the cavitation number of 0.5

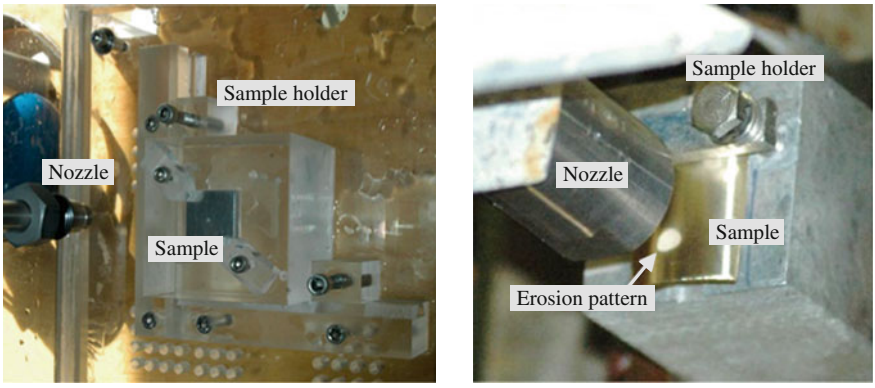

Fig. 2.8 A typical cavitating jet erosion test setup at DYNAFLOW (*left*): the sample is 2.5 cm × 2.0 cm × 2.5 cm. The nozzle diameter is about 2 mm and the standoff distance is about 2.5 cm. The *right picture* shows more specialized testing; here a cylindrically shaped sample is placed under the nozzle. The whole rod piece can be held in place under the jet. The jet and the samples shown in the pictures are submerged in water during the test

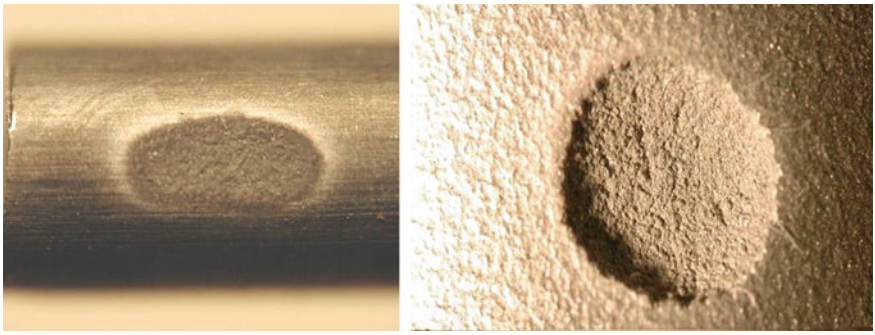

Fig. 2.9 Cavitation erosion pattern on metals created by a CAVIJET® cavitating jet. The *left figure* shows the erosion pattern on the rod sample shown in Fig. 2.8 (*right*), which explains the elliptical shape of the eroded area. The *right picture* shows a more typical erosion pattern on a flat sample. In both pictures the erosion areas had typical size of the order of a centimeter, the samples were surface treated proprietary stainless steels and the jet pressure was about 40 MPa

period of time, (b) the test is interrupted, (c) the sample is taken out from its holder for examination, and (d) the erosion is characterized by weight and depth measurement. Photographs of the progression of the erosion patterns such as shown in Fig. 2.9 are taken at selected times. The sample is then returned for additional testing, and the process is repeated. The time intervals are appropriately selected to capture a cumulative weight loss curve displaying as much as possible the characteristic S-curve (see Chap. 5).

2.4 High-speed Cavitation Tunnels

Cavitation erosion tests can also be conducted in high-speed cavitation tunnels. In order to be able to characterize the resistance to cavitation erosion of hard materials within reasonable exposure times, cavitating flows of sufficiently high aggressiveness are required. As aggressiveness increases with flow velocity, cavitation erosion tunnels are often designed for high velocities and consequently high pressures.

Figure 2.10 presents a typical example of such a facility. The whole facility is designed for a maximum pressure of 4 MPa (40 bar) corresponding to a maximum velocity of about 90 m/s. The facility is equipped with a 80 kW centrifugal pump, which can provide a flow rate of up to 11 l/s. A heat exchanger of 80 kW limits the increase in temperature during long duration tests.

The facility comprises a downstream tank of 1 m^3 pressurized with nitrogen by means of a pressurization vessel. The small section of the pressurization vessel limits the dissolution of nitrogen into water so that the dissolved gas content is expected to be almost independent of the pressurization level. Pressurization is required to control the cavitation number which, in turn, controls the extent of

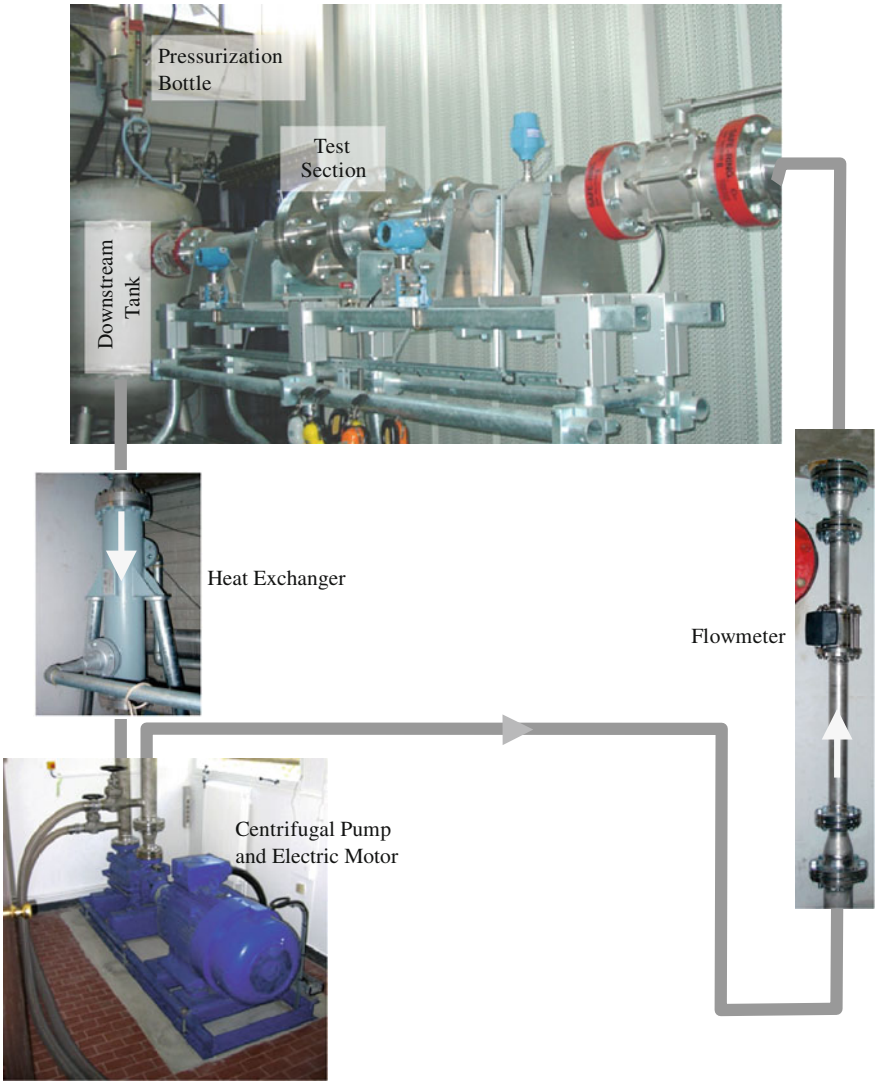

Fig. 2.10 The high-speed cavitation tunnel of the LEGI laboratory (University of Grenoble, France) used for cavitation erosion tests. The tunnel, made of stainless steel, was designed for a maximum operating pressure of 4 MPa (40 bar) corresponding to a maximum flow velocity of 90 m/s. Adapted from [36], with permission from ASME

cavitation and the location of erosion on the sample. In addition, pressurization makes it possible to keep the cavitation number constant when the flow velocity is changed. A similar extent of cavitation is then guaranteed and the effect of flow velocity is separated from the effect of cavitation number or cavity length increase.

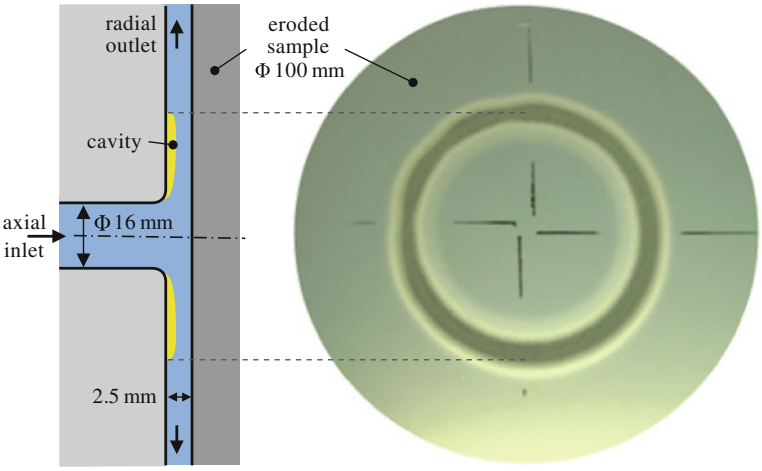

Fig. 2.11 Schematic view of the radial divergent test section used at the LEGI laboratory (University of Grenoble, France) and typical example of an eroded sample. A cavity (*in yellow*) develops at the exit of the 16 mm diameter nozzle, opposite to the sample to be eroded. Erosion is concentrated in the closure region of the cavity and takes the form of a ring due to the axial symmetry of the test section. The mean diameter of the ring is of the order of 45 mm for a value of the cavitation number of 0.9 [37]. Adapted from [36], with permission from ASME

Several pressure sensors are used to control the operating point. A flow meter measures the flow rate Q in the test section and two pressure sensors give the upstream and downstream pressures P_u and P_d respectively. They are located far upstream and downstream of the test section in the inlet and outlet ducts of large diameter (90 mm) with respect to that of the nozzle (16 mm).

The cavitation number is defined by:

$$\sigma = \frac{P_d - P_v}{P_u - P_d}, \tag{2.5}$$

where P_v is the liquid vapor pressure. A temperature sensor is also used to check that the temperature rise during long erosion tests remains limited to typically a few degrees Celsius.

Different types of test sections have been used to investigate cavitation erosion in high-speed tunnels such as a Venturi with or without a central body [25–27], slot cavitator [28–34], cylindrical specimen spanning the tunnel [35] or radial divergent [36].

As an example, the radial divergent test section used in the LEGI ("Laboratoire des Écoulements Géophysiques et Industriels", Grenoble, France) facility is presented in more detail in Figs. 2.11 and 2.12. The inlet flow is axial whereas the outlet flow is radial. Cavitation develops from the nozzle exit and extends into the radial diverging channel. The sample to be eroded faces the nozzle and is located at a distance of 2.5 mm. Cavitation erosion has an annular shape similar to the shape of the closure region of the cavity.

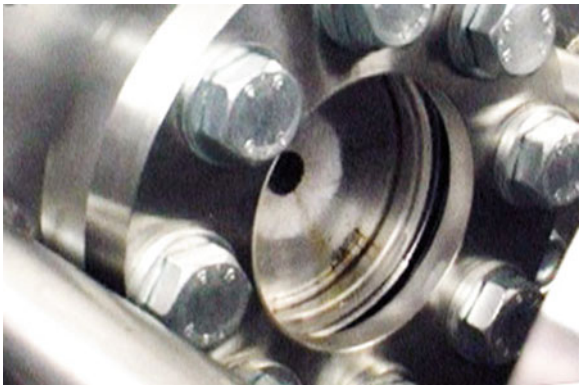

Fig. 2.12 Visualization of the cavity in the radial divergent test section presented in Fig. 2.11. The cavity is the *white* region developing from the 16 mm diameter nozzle exit (*small black circle in the middle*). Flow is from left to right. For visualization purposes, the sample has been replaced by a perspex window, which requires operating the tunnel at a reduced velocity to avoid damage to the window. The value of the cavitation number is 0.9. Adapted from [37], with permission from ASME

For the erosion tests conducted at LEGI, the tunnel is usually operated at a cavitation number around 0.9. With this value of σ, the cavity closure point is located at a radial distance of the order of 22.5 mm from the axis (see Fig. 2.13). Using the definition (2.5) of the cavitation number, the pressure drop through the test section is:

$$P_u - P_d = \frac{P_u - P_v}{1 + \sigma}. \tag{2.6}$$

In this equation, the vapor pressure P_v is generally negligible with respect to the upstream pressure. Since the cavitation number is around 1, Eq. (2.6) shows that the downstream pressure, P_d, in the cavitating test section, and the pressure drop across the nozzle, $P_u - P_d$, are each about half the upstream pressure.

Using Bernoulli equation, a typical velocity on the cavity can be derived:

$$V_c \cong \sqrt{\frac{2P_u}{\rho}}, \tag{2.7}$$

where ρ is the liquid density. Equation (2.7) assumes that the pressure on the cavity surface (which is expected to be close to the vapor pressure) is negligible with respect to the upstream pressure and that the velocity in the inlet duct of large diameter (90 mm) is negligible with respect to the velocity in the test section. As an example, for an upstream pressure of 4 MPa, the velocity on the cavity is $V_c \cong 90\ m/s$. For this typical operating point, the measured flowrate is 8.2 l/s. The equivalent flow velocity in the minimum section area corresponding to the cylindrical section of diameter 16 mm and thickness 2.5 mm at the exit of the

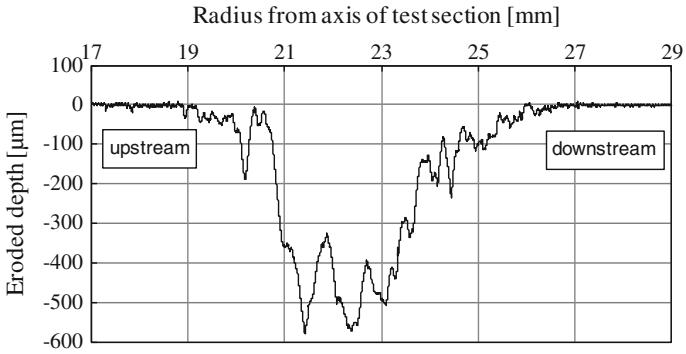

Fig. 2.13 Typical example of a profile of a sample eroded in the cavitation tunnel of the LEGI laboratory. The *horizontal axis* is the radius measured from the center of the test section. The *vertical axis* is the depth of penetration of the damage. Level 0 corresponds to the original non-eroded material surface. Erosion is concentrated in a ring of mean approximate radius 22.5 mm (stainless steel A2205, exposure time: 161 h, upstream pressure: 40 bar, downstream pressure: 18.9 bar, flow rate: 8.2 l/s)

nozzle (see Fig. 2.11) is 65 m/s. This estimate assumes that the flow in this section is purely liquid.

Figure 2.13 presents a typical example of an eroded sample profile along the radial direction. Damage is concentrated in an annular region extending roughly between radius 20 mm and radius 26 mm. The radial location of this region is controlled by the value of the cavitation number. This region moves downstream when the cavitation number is decreased and follows the increase in cavity length.

2.5 Summary

In this chapter, a detailed description of cavitation erosion facilities and equipments was given together with typical measurement results. The facilities include an ultrasonic vibratory horn (G32), a cavitating jet (G134 and its variants) and a high-speed cavitation tunnel with a radial divergent section. They were systematically used to investigate cavitation erosion and the test results are presented in Part I of this book. They include:

- Relatively short duration tests to investigate the cavitation incubation period, various materials pitting, and to deduce impulsive loads on the material (Chap. 3).
- Measurements of the cavitation pressure loads on transducers in order to characterize the amplitude and frequency distribution of cavitation impulsive pressures (Chap. 4).

- Long duration tests to characterize mass loss evolution with time due to cavitation erosion on various materials for different cavitation aggressiveness levels (Chap. 5).

References

1. Billet M (2005) The special committee on cavitation erosion on propellers and appendages on high powered/high speed ships. Paper presented at the 24th International Towing Tank Conference (ITTC), Edinburgh, UK, 4–10 Sept 2005
2. Grekula M, Bark G (2001) Experimental study of cavitation in a kaplan model turbine. Paper presented at the 4th International Symposium on Cavitation (CAV2001), Pasadena, CA, 20–23 Jun 2001
3. Farhat M, Bourdon P (1998) Extending repair intervals of hydro turbines by mitigating cavitation erosion. Paper presented at the CEA Electricity'98 Conference and Exposition, Toronto, 26–29 Apr 1998
4. Farhat M, Bourdon P, Lavigne P, Simoneau R (1997) The hydrodynamic aggressiveness of cavitating flows in hydro turbines. Paper presented at the ASME Fluids Engineering Division Summer Meeting, Vancouver, BC, 22–26 Jun 1997
5. Turbomachinery Society of Japan (2010) Guideline for prediction and evaluation of cavitation erosion in pumps. Tokyo
6. Hammitt FG, Chao C, Kling CL, Mitchell TM, Rogers DO (1970) Round-Robin test with vibratory cavitation and liquid impact facilities of 6061–T 6511 aluminum alloy, 316 stainless steel and commercially pure nickel. Mater Res Stand 10:16–36
7. Chao C, Hammitt FG, Kling CL (1968) ASTM round-robin test with vibratory cavitation and liquid impact facilities of 6061–T6 aluminum alloy, 316 stainless steel, commercially pure nickel, vol 84. The University of Michigan Report MMPP-344-3-T/01357-4-T, Ann Arbor
8. Light KH (2005) Development of a cavitation erosion resistant advanced material system. Master of science thesis, The University of Maine, Orono, ME
9. Dominguez-Cortazar MA, Franc J-P, Michel J-M (1997) The erosive axial collapse of a cavitating vortex: an experimental study. J Fluids Eng 119(3):686–691
10. Hammitt FG (1966) Damage to solids caused by cavitation. Philos Trans R Soc of Lond Ser A Math Phys Sci 260(1110):245–255
11. Escaler X, Avellan F, Egusquiza E (2001) Cavitation erosion prediction from inferred forces using material resistance data. Paper presented at the 4th international symposium on cavitation, Pasadena, California, 20–23 Jun 2001
12. March PA (1987) Evaluating the relative resistance of materials to cavitation erosion: a comparison of cavitating jet results and vibratory results. Paper presented at the ASME cavitation and multiphase flow forum, Cincinnati, 14–17 Jun 1987
13. Momma T, Lichtarowicz A (1995) A study of pressures and erosion produced by collapsing cavitation. Wear 186–187(Part 2):425–436. doi:10.1016/0043-1648(95)07144-x
14. Chahine GL, Courbière P (1987) Noise and erosion of self-resonating cavitating jets. J Fluids Eng 109(4):429–435
15. Lee MK, Kim WW, Rhee CK, Lee WJ (1999) Liquid impact erosion mechanism and theoretical impact stress analysis in tin-coated stream turbine blade materials. Metall Mater Trans A 30A:961–968
16. Pfitsch W, Gowing S, Fry D, Donnelly M, Jessup S (2009) Development of measurement techniques for studying propeller erosion damage in severe wake fields. Paper presented at the 7th international symposium on cavitation (CAV2009), Ann Arbor, Michigan, 17–22 Aug 2009

17. Annual Book of ASTM Standards (2010) Section 3: metals test methods and analytical procedures, vol 03.02. Annual Book of ASTM Standards, West Conshohocken
18. Designation: G 32-09: Standard Test Method for Cavitation Erosion Using Vibratory Apparatus. Annual Book of ASTM Standards (2010) Section 3: Metals test methods and analytical procedures, vol 03.02. West Conshohocken, pp 94–109
19. Hansson I, Mørch KA (1980) The dynamics of cavity clusters in ultrasonic (vibratory) cavitation erosion. J Appl Phys 51(9):4651–4658
20. Designation: G134-95: standard test method for erosion of solid materials by a cavitating liquid Jet. Annual Book of ASTM Standards (2010) Section 3: metals test methods and analytical procedures, vol 03.02, West Conshohocken, pp 558–571
21. Crow SC, Champagne FH (1971) Orderly structure in jet turbulence. J Fluid Mech 48(03):547–591. doi:10.1017/S0022112071001745
22. Johnson VE, Chahine GL, Lindenmuth WT, Conn AF, Frederick GS, Giacchino GJ (1984) Cavitating and structured jets for mechanical bits to increase drilling rate. Part I: theory and concepts. J Energy Res Technol 106(2):282–288
23. Johnson VE, Chahine GL, Lindenmuth WT, Conn AF, Frederick GS, Giacchino GJ (1984) Cavitating and structured jets for mechanical bits to increase drilling rate. Part II: experimental results. J Energy Res Technol 106(2):289–294
24. Chahine GL, Genoux PF (1983) Collapse of a cavitating vortex ring. J Fluids Eng 105(4):400–405
25. Hattori S, Sun B-H, Hammitt FG, Okada T (1985) An application of bubble collapse pulse height spectra to venturi cavitation erosion of 1100-0 aluminum. Wear 103(2):119–131. doi:10.1016/0043-1648(85)90128-0
26. Franc J-P, Michel J-M (1997) Cavitation erosion research in France: the state of the art. J Mar Sci Technol 2:233–244
27. Okada T, Hammitt FG (1981) Cavitation erosion in vibratory and venturi facilities. Wear 69(1):55–69
28. Steller J, Krella A, Koronowicz J, Janicki W (2005) Towards quantitative assessment of material resistance to cavitation erosion. Wear 258(1–4):604–613. doi:10.1016/j.wear.2004.02.015
29. Krella A (2011) An experimental parameter of cavitation erosion resistance for tin coatings. Wear 270(3–4):252–257. doi:10.1016/j.wear.2010.10.065
30. Krella A (2005) Influence of cavitation intensity on X6CrNiTi18-10 stainless steel performance in the incubation period. Wear 258(11–12):1723–1731. doi:10.1016/j.wear.2004.11.025
31. Krella A, Czyzniewski A (2006) Cavitation erosion resistance of Cr–N coating deposited on stainless steel. Wear 260(11–12):1324–1332. doi:10.1016/j.wear.2005.09.018
32. Krella A, Czyzniewski A (2008) Cavitation erosion resistance of nanocrystalline tin coating deposited on stainless steel. Wear 265(7–8):963–970. doi:10.1016/j.wear.2008.02.004
33. Krella A, Czyzniewski A (2009) Cavitation resistance of Cr–N coatings deposited on austenitic stainless steel at various temperatures. Wear 266(7–8):800–809. doi:10.1016/j.wear.2008.11.002
34. Krella A, Czyzniewski A (2007) Influence of the substrate hardness on the cavitation erosion resistance of tin coating. Wear 263(1–6):395–401. doi:10.1016/j.wear.2007.02.003
35. Coleman SL, Scott VD, McEnaney B, Angell B, Stokes KR (1995) Comparison of tunnel and jet methods for cavitation erosion testing. Wear 184(1):73–81. doi:10.1016/0043-1648(94)06563-2
36. Franc J-P (2009) Incubation time and cavitation erosion rate of work-hardening materials. J Fluids Eng 131(2):021303
37. Franc J-P, Riondet M, Karimi A, Chahine GL (2011) Impact load measurements in an erosive cavitating flow. J Fluids Eng 133(12):121301–121308

http://www.springer.com/978-94-017-8538-9

Advanced Experimental and Numerical Techniques for Cavitation Erosion Prediction

Kim, K.-H.; Chahine, G.; Franc, J.-P.; Karimi, A. (Eds.)
2014, XVII, 399 p. 290 illus., 220 illus. in color.,
Hardcover
ISBN: 978-94-017-8538-9